

Distinct Functional MRI Connectivity Patterns and Cortical Volume Variations Associated with Repetitive Blast Exposure in Special Operations Forces Members

Andrea Diociai, MD^{1,2} • Mary A. Iaccarino, MD^{3,4,5,6} • Scott Sorg, PhD⁶ • Emily J. Lubin, BA⁶ • Caroline Wisialowski, BA⁷ • Amol Dua, MD^{1,2} • Can Ozan Tan, PhD⁸ • Rajiv Gupta, PhD^{1,2}

Author affiliations, funding, and conflicts of interest are listed at the end of this article.

See also the editorial by Dogra and Lui in this issue.

Radiology 2025; 315(1):e233264 • <https://doi.org/10.1148/radiol.233264> • Content codes: **NR** **MR**

Background: Special operations forces members often face multiple blast injuries and have a higher risk of traumatic brain injury. However, the relationship between neuroimaging markers, the cumulative severity of injury, and long-term symptoms has not previously been well-established in the literature.

Purpose: To determine the relationship between the frequency of blast injuries, persistent clinical symptoms, and related cortical volumetric and functional connectivity (FC) changes observed at brain MRI in special operations forces members.

Materials and Methods: A cohort of 220 service members from a prospective study between January 2021 and May 2023 with a history of repetitive blast exposure underwent psychodiagnostics and a comprehensive neuroimaging evaluation, including structural and resting-state functional MRI (fMRI). Of these, 212 met the inclusion criteria. Participants were split into two datasets for model development and validation, and each dataset was divided into high- and low-exposure groups based on participants' exposure to various explosives. Differences in FC were analyzed using a general linear model, and cortical gray matter volumes were compared using the Mann-Whitney *U* test. An external age- and sex-matched healthy control group of 212 participants was extracted from the SRPBS Multidisorder MRI Dataset for volumetric analyses. A multiple linear regression model was used to assess correlations between clinical scores and FC, while a logistic regression model was used to predict exposure group from fMRI scans.

Results: In the 212 participants (mean age, 43.0 years \pm 8.6 [SD]; 160 male [99.5%]) divided into groups with low or high blast exposure, the high-exposure group had higher scores for the Neurobehavioral Symptom Inventory (NSI) ($t = 3.16$, $P < .001$) and Posttraumatic Stress Disorder Checklist for *Diagnostic and Statistical Manual of Mental Disorders* (Fifth Edition) (PCL-5) ($t = 2.72$, $P = .01$). FC differences were identified in the bilateral superior and inferior lateral occipital cortex (LOC) (P value range, .001–.04), frontal medial cortex ($P < .001$), left superior frontal gyrus ($P < .001$), and precuneus (P value range, .02–.03). Clinical scores from NSI and PCL-5 were inversely correlated with FC in the LOC, superior parietal lobule, precuneus, and default mode networks ($r = -0.163$ to -0.384 ; P value range, $<.001$ to $.04$). The high-exposure group showed increased cortical volume in regions of the LOC compared with healthy controls and the low-exposure group (P value range, .01–.04). The predictive model helped accurately classify participants into high- and low-exposure groups based on fMRI data with 88.00% sensitivity (95% CI: 78.00, 98.00), 67% specificity (95% CI: 53.00, 81.00), and 73% accuracy (95% CI: 60.00, 86.00).

Conclusion: Repetitive blast exposure leads to distinct alterations in FC and cortical volume, which correlate with neurobehavioral symptoms. The predictive model suggests that even in the absence of observable anatomic changes, FC may indicate blast-related trauma.

© RSNA, 2025

Supplemental material is available for this article.

Traumatic brain injury (TBI) has diverse negative consequences for military personnel, affecting both the structure and function of the brain (1). These effects are especially alarming for special operations forces members, who often face multiple blast injuries. Understanding the long-term neuroimaging implications of repeated blast injuries is challenging due to the variability of injuries in intensity, force, and recurrence, underscoring the multiscale neurologic implications of repeated trauma (2–4). The need for comprehensive studies in this area is underscored by the growing recognition of the persistent and often debilitating effects of repeated blast trauma, such as posttraumatic stress disorder (PTSD), depression, suicidal ideation, cognitive impairments, chronic pain, and an increased risk of brain cancer, which have been associated with moderate, severe, and penetrating TBIs (5). Functional, structural, and molecular neuroimaging techniques, including diffusion-tensor imaging for axonal integrity, resting-state functional MRI (fMRI) for connectivity patterns, and PET for detecting early pathologic changes, have proven valuable in

studying the effects of repetitive low-level blast exposure (6,7), making this population a unique target population for understanding the sequelae of repetitive blast injuries. However, the relationship between neuroimaging markers, the cumulative severity of injury, and long-term symptoms has not previously been well-established in the literature. Understanding these relationships is crucial for developing effective interventions and management strategies for affected individuals. This analysis aimed to determine the relationship between the frequency of blast injuries, persistent clinical symptoms, and related cortical volumetric and functional connectivity (FC) changes observed at brain MRI of active and veteran special operations forces members.

Materials and Methods

Participants

This analysis included 220 participants of the Comprehensive Brain Health and Trauma Program (ComBHaT) at Home Base,

Abbreviations

BEC5 = blast exposure count 5, ComBHAT = Comprehensive Brain Health and Trauma Program, DMN = default mode network, FC = functional connectivity, fMRI = functional MRI, LOC = lateral occipital cortex, NSI = Neurobehavioral Symptom Inventory, PCL-5 = Posttraumatic Stress Disorder Checklist for *Diagnostic and Statistical Manual of Mental Disorders* (Fifth Edition), PTSD = posttraumatic stress disorder, TBI = traumatic brain injury

Summary

In military service members with a history of repetitive blast exposure, higher blast exposure correlated with distinct functional MRI connectivity patterns, changes in cortical volume, and clinical neurobehavioral tests scores; a predictive model indicated possible changes in functional connectivity even in the absence of observable anatomical alterations.

Key Results

- In this analysis of 212 members of special operations forces, participants with higher blast exposure showed altered functional connectivity (FC) in the superior and inferior lateral occipital cortex (LOC), frontal medial cortex, left superior frontal gyrus, and precuneus compared with the low-exposure group (P value range, .001–.04) and had higher cortical volume in the LOC compared with healthy controls and the low-exposure group (P value range, .01–.04).
- Clinical scores from the Neurobehavioral Symptom Inventory and Posttraumatic Stress Disorder Checklist for *Diagnostic and Statistical Manual of Mental Disorders* (Fifth Edition) were inversely correlated with FC in the LOC, superior parietal lobule, precuneus, and default mode networks ($r = -0.163$ to -0.384 ; P value range, $<.001$ to .04).
- Predictive functional MRI modeling classified groups into high or low exposure with 88.00% sensitivity (95% CI: 78.00, 98.00), 67% specificity (95% CI: 53.00, 81.00), and 73% accuracy (95% CI: 60.00, 86.00).

a collaborative initiative between the Red Sox Foundation and Massachusetts General Hospital. Of these 220 participants, 212 met the inclusion criteria. ComBHAT offers a 5-day, multifaceted, and interdisciplinary clinical program to evaluate and treat health and functional concerns in special operations forces military service members and veterans. In this study, we used clinical and neuroimaging data prospectively collected between January 2021 and May 2023. Military status and military branches (eg, Army, Navy SEAL) are shown in Table 1. Additionally, a post hoc analysis included an external age- and sex-matched healthy control group of 212 participants from the SRPBS Multidisorder MRI Dataset (8). The study received institutional review board (IRB) approval and adhered to the Declaration of Helsinki. All data—which were sourced from participants' Home Base–associated medical records and questionnaires—were de-identified at the time of entry into the study database. Written consent was obtained from the first 60 participants (IRB protocol no. 2019P00949). Subsequently, the IRB waived the requirement for written consent for the remaining participants as their collected data were used only for analysis (IRB protocol no. 2022P002143).

The inclusion criteria for enrollment into the ComBHAT program were as follows: (a) being a special operations forces veteran or an active-duty special operations forces service member and (b) referral to the program based on self-reported symptoms. Exclusion criteria for the ComBHAT program included physical and psychiatric conditions requiring a higher level of care, such as current psychotic or manic symptoms, a suicide attempt within the past 90 days, or a current substance use problem necessitating

medical detoxification. For this study, only participants with MRI reports classified as normal by a board-certified neuroradiologist were included, ensuring the absence of structural abnormalities.

Clinical Variables

Participants completed self-report assessments, including the Posttraumatic Stress Disorder Checklist for *Diagnostic and Statistical Manual of Mental Disorders* (Fifth Edition) (PCL-5) (9), Patient Health Questionnaire-8 (10), Neurobehavioral Symptom Inventory (NSI) (11), and Major Depressive Disorder and Generalized Anxiety Disorder questionnaire. Participants were also administered neuropsychological tests like the Full-Scale IQ Test and Wechsler Adult Intelligence Scale Fourth Edition.

The Blast Exposure Threshold Survey was used to assess participants' lifetime blast exposure frequency and intensity, representing cumulative exposure from all military weapons and explosives (12) (Fig S1).

Neuroimaging

Brain MRI was performed using 3-T Siemens Magnetom Skyra and Vida machines. We obtained both structural and resting-state fMRI data. The specific imaging parameters and sequences are provided in Table S1. All fMRI data underwent processing using CONN (13) (RRID:SCR_009550) release 21.a and SPM (14) (RRID:SCR_007037) release 12.7771. A detailed preprocessing pipeline was applied to the functional and anatomic images (15), with specifics available in Appendix S1 (Preprocessing section).

Imaging Analysis

All MRI scans were reviewed by a board-certified neuroradiologist (R.G.) with 20 years of experience, revealing no visually recognizable blast-related alterations. We divided the data from 212 participants into two datasets. Dataset 1 comprised the first 161 sequentially enrolled participants, split into high and low blast exposure groups based on a median blast exposure count 5 (BEC5) score of 1800, similar to what was previously performed by Edlow et al (16). We used dataset 1 as a set to derive patterns distinguishing these groups. Dataset 2 included the next 51 participants, enrolled after we completed analysis of dataset 1. Dataset 2 served as a surrogate group to assess the consistency of the findings. A bootstrap analysis helped confirm the consistency of results between datasets (Table S2). The median BEC5 value from the first dataset was used for the second dataset to have a common separator threshold that is not biased by group-to-group differences. The use of different median values would have led to divergent separation boundaries between the datasets, making them noncomparable. A visual division of the datasets is provided in Figure 1.

Due to the unique composition of our cohort, all special operations forces members, including those outside the ComBHAT program, have blast exposure and cannot serve as an unexposed control group. Instead, we analyzed the impact of exposure burden within our sample. Methodology and imaging protocols are detailed in Appendix S1 (MRI Acquisition and Preprocessing section).

First-level analysis.—In neuroimaging, FC is defined as the correlations between brain region activities over time and is indicative of functional interaction. In our study, we used multivariate pattern analysis to examine voxel activation patterns and seed-based connectivity to assess FC differences across seed areas (17).

Table 1: Demographic Characteristics and Clinical Scores for Both Datasets

Characteristic	Dataset 1 (n = 161)	Dataset 2 (n = 51)	All Participants (n = 212)
Male	160 (99.53)	51 (100.00)	211 (99.53)
Age (y)*	43.03 ± 8.57	42.76 ± 8.56	43.00 ± 8.56
No. of deployments*	7.55 ± 6.31	8.37 ± 7.14	7.75 ± 6.5
Race			
White	156 (96.89)	49 (96.08)	205 (96.70)
Asian	2 (1.24)	1 (1.96)	3 (1.42)
Black	1 (0.62)	1 (1.96)	2 (0.94)
Pacific Islander	1 (0.62)	0 (0.00)	21 (0.95)
Other	1 (0.62)	0 (0.00)	1 (0.47)
Military status			
Active duty	120 (74.53)	23 (45.10)	143 (67.45)
Discharged	20 (12.42)	24 (47.06)	44 (20.75)
Retired	17 (10.56)	2 (3.92)	19 (8.96)
National Guard	2 (1.24)	1 (1.96)	3 (1.42)
Reserve	1 (0.62)	1 (1.96)	2 (0.94)
Medically retired	1 (0.62)	0 (0.00)	1 (0.47)
Branch			
Navy SEAL	69 (42.86)	13 (25.49)	82 (38.68)
NSW	11 (6.83)	3 (5.88)	14 (6.60)
SWCC	11 (6.83)	2 (3.92)	13 (6.13)
Navy EOD	10 (6.21)	4 (7.84)	14 (6.60)
MARSOC	3 (1.86)	0 (0.00)	3 (1.42)
Green Beret	6 (3.73)	4 (7.84)	10 (4.72)
Army	5 (3.11)	12 (23.53)	17 (8.02)
Navy	4 (2.48)	8 (15.69)	12 (5.66)
Ranger	2 (1.24)	0 (0.00)	2 (0.94)
EOD	23 (14.29)	0 (0.00)	23 (10.85)
JSOC	9 (5.59)	0 (0.00)	9 (4.25)
AFSOC	4 (2.48)	5 (9.80)	9 (4.25)
Night Stalker	2 (1.24)	0 (0.00)	2 (0.94)
Other	2 (1.24)	0 (0.00)	2 (0.94)
Clinical scores*			
NSI	31.45 ± 19.38	28.29 ± 16.48	30.70 ± 18.73
NSI Vestibular	3 ± 2.65	2.37 ± 2.17	2.84 ± 2.54
NSI Somatic	8.92 ± 5.77	8.09 ± 4.12	8.70 ± 5.4
NSI Affective	10.99 ± 6.01	11.09 ± 5.13	11.01 ± 5.79
NSI Cognitive	7.83 ± 4.45	6.74 ± 4.05	7.55 ± 4.37
PROMIS Ability	11.37 ± 3.71	11.57 ± 3.32	11.41 ± 3.61
FSIQ	113.11 ± 10.65	112.72 ± 9.33	113.02 ± 10.36
VCI	113.01 ± 11.10	112.62 ± 10.85	112.92 ± 11.02
PRI	113.88 ± 12.20	112.48 ± 12.41	113.55 ± 12.24
WMI	107.06 ± 13.03	108.53 ± 12.21	107.41 ± 12.83
PSI	105.64 ± 12.71	105.61 ± 13.34	105.63 ± 12.84
PCL-5	33.33 ± 18.90	30.70 ± 13.81	32.77 ± 17.77

Note.—Except where indicated, data are numbers of participants, with percentages in parentheses. AFSOC = Air Force Special Operations Command; EOD = Explosive Ordnance Disposal; FSIQ = Full-Scale IQ Test; Green Beret = U.S. Army Special Forces; JSOC = Joint Special Operations Command; MARSOC = Marine Forces Special Operations Command; Navy SEAL = U.S. Navy Sea, Air, and Land Teams; Night Stalker = 160th Special Operations Aviation Regiment (Airborne); NSI = Neurobehavioral Symptom Inventory; NSW = Naval Special Warfare; Other = other military special operations personnel; PCL-5 = Posttraumatic Stress Disorder Checklist for *Diagnostic and Statistical Manual of Mental Disorders* (Fifth Edition); PRI = Perceptual Reasoning Index; PROMIS = Patient Reported Outcomes Measurement Information System; PSI = Processing Speed Index; Ranger = U.S. Army Ranger Regiment; SWCC = Special Warfare Combatant-Craft Crewmen; VCI = Verbal Comprehension Index, WMI = Working Memory Index.

* Data are means ± SDs.

Group-level analyses.—A general linear model was applied to voxel-wise first-level connectivity measures. Multivariate parametric statistics were used to assess variable interactions, with cluster-level

inferences based on Gaussian random field theory (18). A stringent threshold system was used to minimize false positives. These analyses are detailed in Appendix S1 (Second-level analysis section).

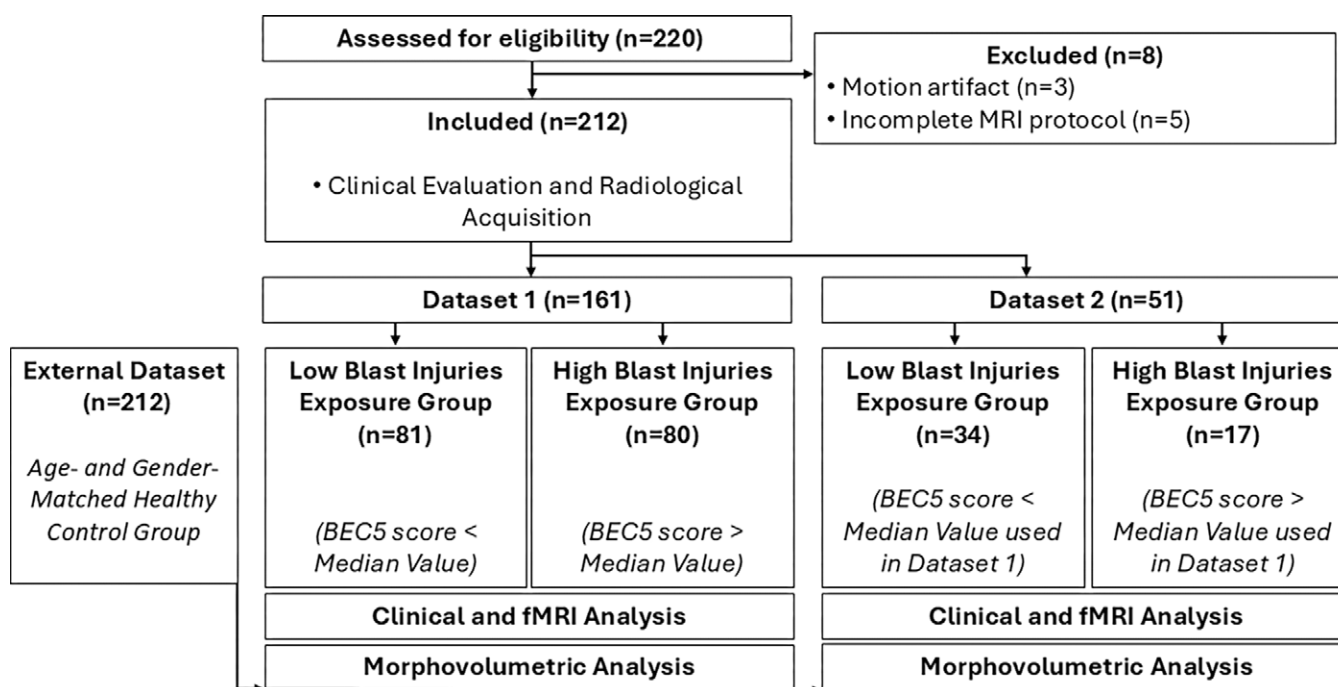


Figure 1: Flowchart depicts participant selection, dataset division, and analysis pipeline. A total of 220 participants were initially assessed for eligibility. Eight participants were excluded due to motion artifacts ($n = 3$) or incomplete MRI protocols ($n = 5$), resulting in a final sample of 212 participants. The cohort was divided into two datasets: dataset 1 ($n = 161$) and dataset 2 ($n = 51$). Each dataset was further stratified into low and high blast injury exposure groups based on the median blast exposure count 5 (BEC5) value from dataset 1. Dataset 2 was used as an independent validation set, employing the same median BEC5 threshold as dataset 1. Analyses included clinical assessments, functional MRI (fMRI) connectivity analysis, and morphovolumetric evaluations. Additionally, an external age- and sex-matched healthy control group ($n = 212$) was incorporated for volumetric comparisons.

Volumetric analyses.—Gray matter volume was extracted from the lateral occipital cortex (LOC) delineated by using the Harvard-Oxford Atlas and normalized by label median and total gray matter volume. Statistical tests were performed separately for each dataset to assess volume differences across participant groups. A post hoc analysis included an age- and sex-matched healthy control group ($n = 212$) (8). Technical processes are provided in Appendix S1 (Volumetric Analysis section).

Statistical Analysis

Neuropsychological tests were compared between high- and low-exposure groups using a two-sided t test, with effect sizes quantified using the Cohen d test. The primary analysis used BEC5 as the independent variable, with sensitivity analyses substituting BEC2 and generalized blast exposure value (Fig S2). Statistical analyses were conducted by an author (A. Diociasi) using Jamovi 2.3.28.

To assess major depressive disorder, generalized anxiety disorder, and PTSD relative to BEC5, blast exposure count 2 (ie, BEC2), and generalized blast exposure value, a logistic regression model was used. A multiple linear regression model was employed to explore the relationships between NSI, PCL-5, and FC, specifically adjusting for the impact of BEC5.

For further validation, a method was devised to predict participant groups using only fMRI scans. We employed a logistic regression model to differentiate between high- and low-exposure groups. All 212 participants were categorized on the basis of their median BEC5 score, that is, whether it was above or below the median. This categorization was the dependent variable. For predictive variables, we selected regions of interest

from the CONN second-level analysis results encompassing both superior and inferior LOCs as well as medial frontal cortex and precuneus. Sensitivity, specificity, and accuracy were calculated. The procedure for extracting voxel time series from the relevant regions is detailed in Appendix S1 (Extraction of Voxel Time Series section).

In the volumetric study, the Mann-Whitney U test was performed to compare normalized volumes across BEC5 groups, with $P < .05$ indicating a statistically significant difference (Table 2, Fig S4). Each dataset was analyzed separately, and a post hoc analysis included an age-matched healthy control group.

Results

Participant Characteristics

The initial sample included 220 participants, of whom eight were excluded due to motion artifacts on fMRI images or incomplete imaging protocols. Thus, the final cohort was comprised of 212 participants, as depicted in Figure 1. The sample was predominantly male (99.53%) and White (96.70%), with a majority still serving on active duty (67.45%) and a mean age of 43.00 years \pm 8.56 (SD). Characteristics of the participants are detailed in Table 1.

Clinical Variables

In dataset 1, higher clinical scores were observed for the high blast exposure group in comparison with the low blast exposure group, indicating more severe symptoms on the NSI ($t = 3.16$; Cohen $d = 0.50$; mean difference = 8.68; SE = 2.75; 95% CI = 3.26, 14.11), Patient Health Questionnaire-8 ($t = 2.47$;

Table 2: Comparison of Cortical Volumes between Higher and Lower Large Explosive Exposure Groups

Dataset and Region of Interest	Volume (mm ³)		<i>P</i> Value	Cohen <i>d</i> Value
	Lower Large Explosive Exposure Group	Higher Large Explosive Exposure Group		
Dataset 1				
Right superior LOC	19 166 ± 190.4	19 431 ± 210.0	.016*	0.10
Left superior LOC	18 911 ± 187.7	19 550 ± 209.0	.018*	0.19
Right inferior LOC	10 030 ± 81.0	10 182 ± 80.2	.025*	0.18
Left inferior LOC	9358 ± 82.0	9569 ± 92.1	.062	0.14
Dataset 2				
Right superior LOC	18 616 ± 257	19 413 ± 483	.029*	0.33
Left superior LOC	18 928 ± 273	20 164 ± 500	.034*	0.32
Right inferior LOC	9875 ± 117	9825 ± 210	.247	0.12
Left inferior LOC	9236 ± 109	9862 ± 211	.019*	0.36

Note.—The results demonstrate that individuals with higher exposure to large explosions had significantly larger volumes in the superior and inferior lateral occipital cortex (LOC) compared with those with lower exposure. The null hypothesis ($H_0: \mu_0 = \mu_1$) was initially tested for each of the four regions separately. Based on significant findings, the alternative hypothesis ($H_a: \mu_0 < \mu_1$) was formulated to further confirm and interpret the observed differences. These findings suggest a potential relationship between blast exposure and LOC volume differences ($H_a: \mu_0 < \mu_1$). Median values of normalized volume (\pm SEs) are reported. *P* values are calculated with the Mann-Whitney *U* test.

* $P < .05$.

Table 3: Differences in Clinical Scores between Participants of Dataset 1 Separated according to the Median BEC5

Test	<i>T</i> Statistic	<i>P</i> Value	Cohen <i>d</i> Value	Mean Difference ± SE	95% CI
NSI	3.16	<.001*	0.50	8.68 ± 2.75	3.26, 14.11
NSI Vestibular	2.19	.03*	0.35	0.88 ± 0.40	0.09, 1.68
NSI Somatic	3.13	.02*	0.50	2.67 ± 0.85	0.98, 4.35
NSI Affective	2.77	.01*	0.44	2.51 ± 0.91	0.72, 4.30
NSI Cognitive	2.35	.02*	0.38	1.61 ± 0.68	0.26, 2.96
PROMIS Ability	−0.82	.41	−0.13	−0.46 ± 0.55	−1.55, 0.64
FSIQ	0.79	.43	0.13	8.99 ± 11.36	−13.44, 31.43
PHQ	2.47	.01*	0.39	2.31 ± 0.94	0.46, 4.16
PCL-5	2.72	.01*	0.43	7.81 ± 2.86	2.15, 13.46
VCI	−1.26	.21	−0.20	−2.22 ± 1.77	−5.71, 1.27
PRI	0.07	.95	0.01	0.13 ± 2.03	−3.87, 4.14
WMI	0.64	.53	0.10	7.37 ± 11.51	−15.36, 30.10
PSI	0.81	.42	0.13	9.36 ± 11.51	−13.37, 32.09

Note.—The table shows that participants with higher blast exposure had significantly higher NSI total and subscale scores, as well as higher PHQ and PCL-5 scores, indicating more severe neurobehavioral and psychologic symptoms. BEC5 = blast exposure count 5, FSIQ = Full-Scale Intelligence Quotient, NSI = Neurobehavioral Symptom Inventory, PCL-5 = Posttraumatic Stress Disorder Checklist for *Diagnostic and Statistical Manual of Mental Disorders* (Fifth Edition), PHQ = Patient Health Questionnaire, PRI = Perceptual Reasoning Index, PROMIS = Patient-Reported Outcomes Measurement Information System (Physical Function–Ability), PSI = Processing Speed Index, VCI = Verbal Comprehension Index, WMI = Working Memory Index. *P* values were determined using an independent samples *t* test. For the bootstrap analysis of clinical differences, please refer to Table S2.

* = Statistically significant.

Cohen *d* = 0.39; mean difference = 2.31; SE = 0.94; 95% CI = 0.46, 4.16), and PCL-5 ($t = 2.72$; Cohen *d* = 0.43; mean difference = 7.80; SE = 2.86; 95% CI = 2.15, 13.46). Correlations between clinical variables and groups are shown in Table 3 and Figure S2.

No significant associations were found between generalized anxiety disorder, major depressive disorder, PTSD, and blast exposure count measures at logistic and linear regression analyses. While generalized anxiety disorder showed a significant correlation, the model had a poor fit ($R^2 = 0.003$; root mean square error = 21 587; 95% CI for generalized anxiety disorder = 0.11, 1.07), indicating minimal explanatory power.

Imaging Analysis

A second-level FC–multivariate pattern analysis was performed on MRI scans from dataset 1, separating participants into two groups based on median BEC5 score. This analysis revealed some clusters that showed differences in mean connectivity between the groups (contrast 1, −1) in both datasets. The clusters involved bilateral superior and inferior LOCs (*P* value range, .001–.04), the frontal medial cortex ($P < .001$), left superior frontal gyrus ($P < .001$), and precuneus (*P* value range, .02–.03) (Figs 2, 3).

A multiple regression analysis was conducted to assess the effects of NSI and PCL-5 scores on connectivity in relation to blast

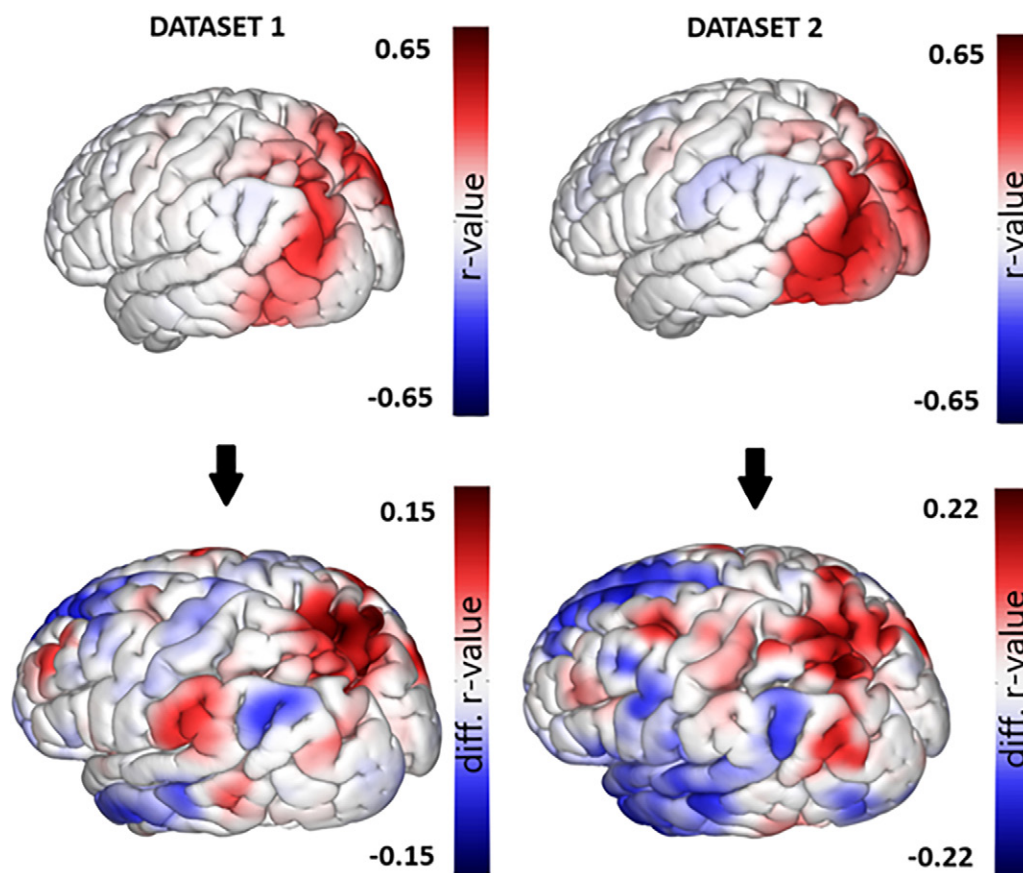


Figure 2: Upper panel displays functional MRI (fMRI) maps obtained from the functional connectivity multivariate patterns analysis conducted on dataset 1 and dataset 2. In particular, the average connectivity across all participants is illustrated with one of the clusters that showed differences between the groups. The colors depict the r value ranging from red to blue. Cluster (x,y,z) selected for datasets 1 and 2 were centered, respectively, at $(+36, -66, +24)$ and $(+30, -84, +16)$. For a comprehensive overview of all clusters displaying statistically significant differences among groups, please refer to Figure 3. Images in bottom panel highlight the differences between groups (color coded from red to blue), focusing on the same cluster chosen as a seed in the top row. The average connectivity is illustrated with the contrasted cluster across participants (diff. r -value) (contrast 1, -1), showing a comparable disparity between the two datasets. Cluster-level inferences based on Gaussian random field theory (18), cluster threshold $P < .05$, cluster-size P value false discovery rate corrected; voxel threshold: $P < .001$, P value uncorrected.

exposure. A subsequent post hoc analysis was performed to examine the correlation between clinical scores and BEC5 using the Pearson correlation coefficient. This deeper investigation highlighted seed regions where clinical scores tended to have varying effects on FC. Specifically, the NSI score was negatively correlated with FC between the bilateral superior LOC and the left superior parietal lobe (Pearson $r = -0.174$ and -0.163 for the left superior LOC and right superior LOC, respectively; $P = .04$) (Fig 4). The PCL-5 score demonstrated a negative correlation with FC in the superior LOC and regions including the precuneus, supramarginal gyrus (right), and bilateral pre- and post-central gyri (Pearson $r = -0.283$, $P < .001$) (Fig 5, top row).

In addition, the PCL-5 score was negatively correlated with FC between default mode networks (DMNs) (posterior cingulate cortex, lateral parietal left, lateral parietal right, and medial prefrontal cortex) and regions involving the left superior LOC, angular gyrus, supramarginal gyrus, frontal pole, and paracingulate cortex (Pearson $r = -0.384$, $P < .001$) (Fig 5, bottom row).

Across varied analytical methods, including multivariate pattern analysis and seed-based connectivity analysis, distinct clusters and regions with connectivity disparities were consistently identified between the groups.

To substantiate these findings, an internal pipeline was devised to help predict participants' exposure group (ie, high or low exposure to large explosives) based purely on fMRI signals sourced from the regions of interest, which demonstrated group disparities involving right superior LOC, left superior LOC, right inferior LOC, left inferior LOC, precuneus, and medial frontal cortex. Dataset 1 was split into an 80:20 training-validation ratio before testing on dataset 2. When tested on the dataset 1 validation subset ($n = 32$), this pipeline had a sensitivity of 80.00% (26 of 32; 95% CI: 74.00, 86.00), specificity of 74.00% (24 of 32; 95% CI: 67.00, 81.00), and accuracy of 76.00% (24 of 32; 95% CI: 69.00, 82.00). Testing on the external validation set (dataset 2, $n = 51$) resulted in a sensitivity of 88.00% (45 of 51; 95% CI: 78.00, 98.00), specificity of 67.00% (34 of 51; 95% CI: 53.00, 81.00), and accuracy of 73.00% (37 of 51; 95% CI: 60.00, 86.00).

Following the fMRI analysis, a volumetric study for each dataset was independently executed. Both investigations revealed that participants with higher exposure to significant explosives (garnering a higher BEC5 subscore) possessed an increased volume in the left and right superolateral occipital cortices. Specifically, in dataset 1, the higher exposure group showed significantly greater volumes in the right superior LOC (median, 19431 mm³

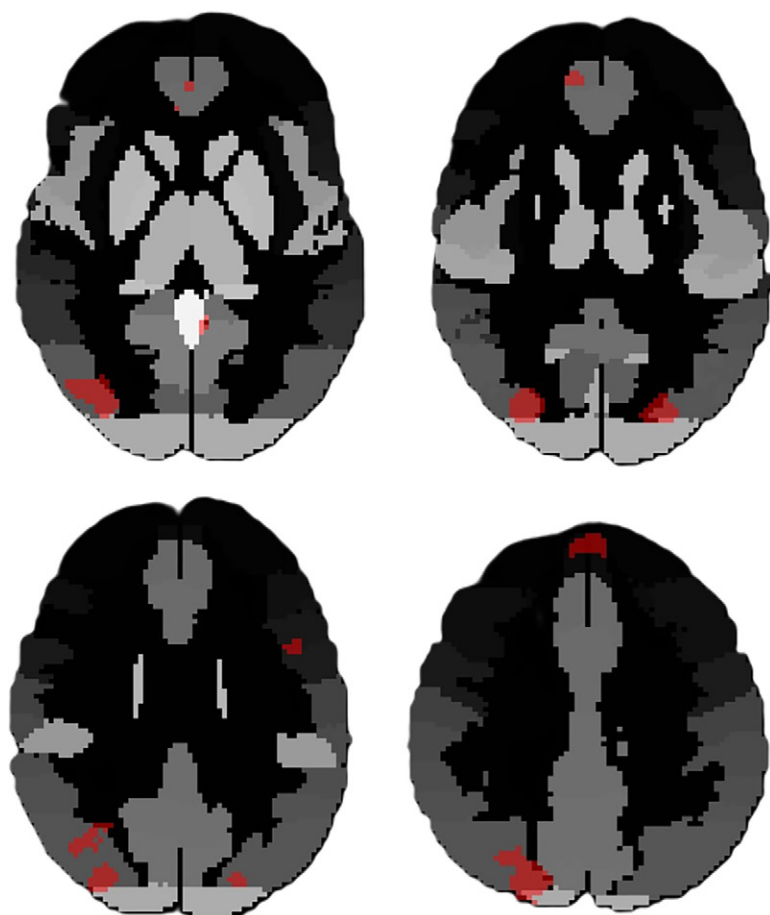


Figure 3: Functional MRI (fMRI) scans depict the merged regions of interest that showed significant differences between the high and low blast exposure groups in both dataset 1 and dataset 2. These regions of interest were combined to create a unified representation of the second-level analysis. These regions were used in the model to predict group membership solely based on fMRI data. The clusters involved the bilateral superior and inferior lateral occipital cortex, the frontal medial cortex, left superior frontal gyrus, and precuneus.

± 210.0 [SE] vs $19\,166\text{ mm}^3 \pm 190.4$, respectively; $P = .016$) and left superior LOC (median, $19\,550\text{ mm}^3 \pm 209.0$ vs $18\,911\text{ mm}^3 \pm 187.7$; $P = .018$) compared with the lower exposure group. Similarly, the right inferior LOC (median volume, $10\,182\text{ mm}^3 \pm 80.2$ vs $10\,030\text{ mm}^3 \pm 81.0$; $P = .025$) and left inferior LOC (median volume, $9\,569\text{ mm}^3 \pm 92.1$ vs $9\,358 \pm 82.0$; $P = .062$) followed the same trend. In dataset 2, the median volume in the right superior LOC ($19\,413\text{ mm}^3 \pm 483$ vs $18\,616\text{ mm}^3 \pm 257$; $P = .029$) and left superior LOC ($20\,164\text{ mm}^3 \pm 500$ vs $18\,928\text{ mm}^3 \pm 273$; $P = .034$) were again larger in the higher exposure group. The median volume in the right inferior LOC ($9\,825\text{ mm}^3 \pm 210$ vs $9\,875\text{ mm}^3 \pm 117$, $P = .247$) showed no significant difference, while that in the left inferior LOC ($9\,862\text{ mm}^3 \pm 211$ vs $9\,236\text{ mm}^3 \pm 109$, $P = .019$) was significantly larger (Table 2, Fig S3). Furthermore, the group with higher exposure showed significant volumetric differences compared with healthy controls, particularly in the left superior LOC (median, $19\,536\text{ mm}^3 \pm 1902$ vs $18\,906\text{ mm}^3 \pm 2432$, respectively; $P = .032$), right inferior LOC (median, $10\,026\text{ mm}^3 \pm 743$ vs $9\,775\text{ mm}^3 \pm 955$; $P = .020$), and left inferior LOC (median, $9\,510\text{ mm}^3 \pm 832$ vs $9\,326\text{ mm}^3 \pm 935$; $P = .054$).

In contrast, the lower BEC5 exposure group showed no significant differences from healthy controls across all regions (P

value range, .30–.91) (Fig S4). The functional study pinpointed the engagement of the LOC within clusters that displayed connectivity differences between participants sorted according to high and low BEC5 scores. A similar analysis was also conducted using the generalized blast exposure value to divide the groups, yielding consistent results. However, when using the generalized blast exposure value metric to classify groups across different databases, volume differences were not consistently evident.

Discussion

This study examined the effects of repetitive blast exposure on functional connectivity (FC) and cortical volume in 212 special operations forces members, revealing distinct neuroimaging and clinical patterns. Participants with high blast exposure exhibited altered FC in the superior and inferior lateral occipital cortex (LOC), frontal medial cortex, left superior frontal gyrus, and precuneus (P value range, $<.001$ –.04). Cortical volume was significantly larger in the LOC for high-exposure participants compared with both low-exposure individuals and an external healthy control group (P value range, .01–.04). Higher blast exposure correlated with increased neurobehavioral symptoms, as measured by the Neurobehavioral Symptom Inventory ($t = 3.16$, $P < .001$) and Posttraumatic Stress Disorder Checklist for *Diagnostic and Statistical Manual of Mental Disorders* (Fifth Edition) ($t = 2.72$, $P = .01$). Clinical scores were inversely correlated with FC in regions linked to cognition, attention, and emotional regulation, including the LOC, superior parietal lobule, precuneus, and default mode network (Pearson r range, -0.163 to -0.384 ; P value range, $<.001$ to .04). A predictive functional MRI model helped accurately classify participants into high- or low-exposure groups with 88.00% sensitivity (95% CI: 78.00, 98.00), 67% specificity (95% CI: 53.00, 81.00), and 73% accuracy (95% CI: 60.00, 86.00).

Resting-state fMRI has emerged as a powerful tool for assessing trauma-related brain changes. Prior research demonstrated 95.83% accuracy in identifying mild TBI using fMRI and PET (19). Harnett et al (20) demonstrated that resting-state fMRI performed shortly after trauma could help predict future PTSD and depression symptoms. Similarly, Zhang et al (21) showed that resting-state fMRI can help predict responses to treatment in patients with major depressive disorder. These findings underscore the potential of resting-state MRI as a biomarker for trauma exposure and treatment response. Our results align with these findings. In our cohort, we were able to further investigate the impact of blast exposure on FC and successfully classify participants into higher or lower exposure groups.

Earlier studies, which were limited by small sample sizes (<20 patients), identified cumulative damage in similar populations (22). With our larger cohort, we confirmed altered connectivity in the LOC, precuneus, medial frontal cortex, and inferior frontal gyrus in participants with high BEC5, likely due to recurrent minor blast injuries. Additionally, LOC cortical volume was significantly larger in high-exposure participants across both datasets

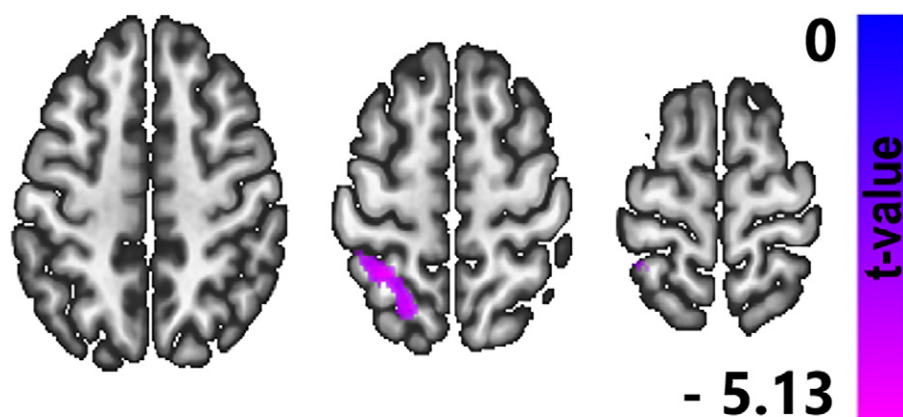


Figure 4: Functional MRI scans highlight the effect of Neurobehavioral Symptom Inventory (NSI) score on functional MRI connectivity while controlling for median blast exposure count 5 value and using lateral occipital cortices as the reference seed. NSI demonstrates a negative correlation with functional connectivity between the seed regions (lateral occipital cortices) and a cluster centered in the left superior parietal lobule (Pearson $r = -0.174$ and -0.163 for left and right superior lateral occipital cortices, respectively; $P = .04$), suggesting that higher symptom severity is linked to weaker communication between these brain regions.

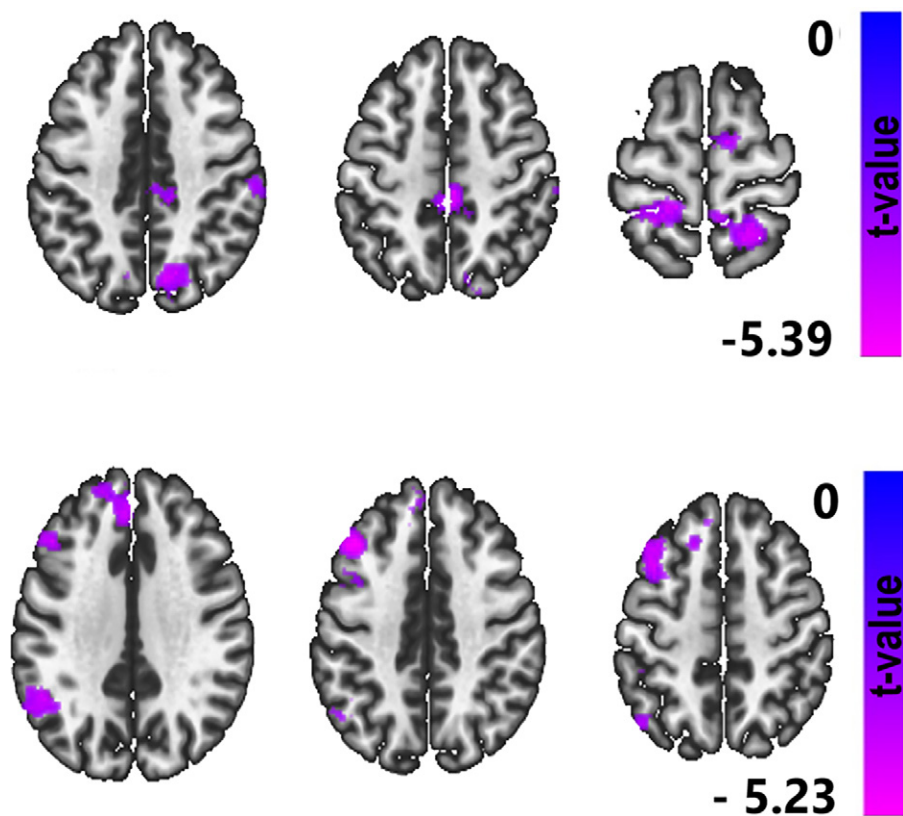


Figure 5: Functional MRI (fMRI) scans highlight the effect of the Posttraumatic Stress Disorder Checklist for Diagnostic and Statistical Manual of Mental Disorders (Fifth Edition) (PCL-5) score on fMRI connectivity while controlling for blast exposure count 5 value using as the reference seeds the precuneus (top row) and default node networks (DMNs) (posterior cingulate cortex, lateral parietal left, lateral parietal right, medial prefrontal cortex) (bottom row), suggesting that greater posttraumatic stress disorder symptom severity is associated with weaker connections in brain regions involved in attention, memory, and emotional regulation. Pearson correlation analysis showed that NSI is negatively correlated with functional connectivity (FC) between superior lateral occipital cortices (LOCs) and regions involving precuneus, right supramarginal gyrus, and bilateral pre- and post-central gyrus (Pearson $r = -0.283$, $P < .001$). Furthermore, PCL-5 is negatively correlated with FC between the DMNs (posterior cingulate cortex, lateral parietal left, lateral parietal right, medial prefrontal cortex) and areas involving the left superior LOC, left angular gyrus, and left supramarginal gyrus, as well as left frontal pole and paracingulate areas (Pearson $r = -0.384$, $P < .001$).

and was further validated with an external control group. Other investigators have noted an increased volume and surface area in the LOC, which showed an inverse relationship with the performance on the Trail Making Test part A (23). While standard MRI protocols often miss mild TBI-related damage, advanced techniques like diffusion-tensor imaging and morphometric volumetric analysis can better depict these microstructural changes (24).

Historical data suggest that experienced breachers (operational personnel who receive specialized training to gain entry through hardened structures) display thicker cortices in the occipital lobe and DMN, coupled with radial diffusivity and fractional anisotropy variations, possibly indicating diminished myelination and astroglial scarring (25). Crombie et al (26) linked LOC thickness to PTSD symptom severity, while previous studies reported reduced perfusion in LOC regions in patients with mild TBI (27). Interestingly, we found a correlation between PTSD symptoms and FC in areas previously associated with FC PTSD-related alterations, such as the precuneus, pre- and postcentral gyri, and the frontal pole, which in part overlaps with the medial prefrontal cortex. These findings are consistent with the results of the meta-analysis by Bao et al (28), highlighting disrupted connectivity in these regions as hallmark features of PTSD.

Interestingly, our analysis shows that participants with higher blast exposure had elevated NSI and PCL-5 scores, both of which are widely used in assessing mild TBI in military personnel (29,30). The NSI is used to assess various domains, including affective, cognitive, somatosensory, and vestibular functions (Table 1). Pearson correlation analysis revealed a negative correlation between NSI score and FC in specific brain regions. Interestingly, these regions appear to overlap with areas implicated in the same domains to varying degrees (31,32). Our findings not only highlight differences in clinical scores between groups but also reveal that these clinical scores have a significant influence on FC. These findings suggest that blast-related FC changes are not merely correlational but modulated by symptom severity,

reinforcing the impact of repeated blast exposure on brain connectivity in clinically relevant regions (33).

The precuneus, a key DMN component, plays a central role in processing external and internal information (34). Moreover, the LOC, beyond its essential function in object recognition (35,36), has been associated with the appreciation of aesthetic artworks, underlining its multifaceted role (37).

Earlier studies have reported mixed findings on DMN connectivity patterns following TBIs, with evidence of both hypoconnectivity and hyperconnectivity across different studies. Mayer et al (38) found initial DMN hypoconnectivity after trauma with no significant abnormalities at 4 months. Iraj et al (39) reported similar hypoconnectivity in patients with mild TBI. Hypoconnectivity has also been noted in PTSD and TBI, highlighting the complex effects of trauma on connectivity (28). Bao et al (28) linked DMN hypoconnectivity to both trauma and PTSD, with dorsal DMN alterations present even in trauma-exposed individuals without PTSD. This indicates that trauma exposure alone may lead to enduring changes in the DMN, which aligns with our results. Even in the absence of a statistically significant correlation between PTSD and blast exposure, the relationship between PTSD symptoms (PCL-5), FC, and trauma exposure aligns with the expected pattern, supporting the notion that blast exposure could indeed influence both clinical symptoms and FC.

Our study has some limitations. Our fMRI analysis lacks a control group of individuals without blast injuries due to the unique nature of our cohort. Given their training and exposure, finding an appropriate “non-TBI” control within their ranks was challenging. To address this, we studied the dose-dependent nature of TBI and used the second dataset as a surrogate “control group.” A post hoc volumetric analysis also incorporated an age-matched healthy control group. Another limitation is the reliance on self-reported BEC5 scores, which may introduce recall bias. Additionally, data on comorbidities were not included in the analyses. Our decision to bifurcate datasets based on the median BEC5 score followed prior studies (13) but remains somewhat arbitrary and lacks randomization, potentially leading to varied outcomes across samples. To minimize bias and validate findings, we applied the same BEC5 threshold to dataset 2 and performed bootstrap analysis, ensuring consistency.

In conclusion, our investigation showed that participants with heightened exposure to significant large explosives (eg, blast exposure count 5)—surpassing the median threshold—manifest distinct functional MRI (fMRI) connectivity patterns compared with their counterparts with lesser exposure. Our study sample exhibited variations in the cortical volume, specifically within regions that the fMRI analysis identified as markedly different between the groups. These comparative cortical volumetric results were consistent when an external age-matched healthy control group was used. Furthermore, clinical metrics like the Neurobehavioral Symptom Inventory and Posttraumatic Stress Disorder Checklist for *Diagnostic and Statistical Manual of Mental Disorders* (Fifth Edition) scores rise in tandem with increasing blast exposure and are inversely correlated with functional connectivity (FC) in those very regions, showing divergent FC patterns and volume differences. Our study also successfully modeled and predicted binarized blast exposure level using only the fMRI data. The aim of this modeling was to underscore the idea that the traumatic effects of blasts can cause shifts in FC, even when anatomic

alterations are not evident at conventional MRI. This method may bridge the existing divide between clinical observations and imaging outcomes in participants exposed to blasts. Future studies should use advanced models integrating multimodal imaging to enhance detection of subtle blast-induced neural changes.

Deputy Editor: Sven Haller

Scientific Editor: Kate Vilas

Author affiliations:

¹ Department of Radiology, Mass General Brigham, Massachusetts General Hospital, Boston, Mass

² Department of Radiology, Massachusetts General Hospital, Harvard Medical School, 55 Fruit St, Boston, MA 02114-2605

³ Department of Physical Medicine and Rehabilitation, Harvard Medical School, Charlestown, Mass

⁴ Department of Physical Medicine and Rehabilitation, Harvard Medical School, Boston, Mass

⁵ Department of Physical Medicine and Rehabilitation, Spaulding Rehabilitation Hospital Boston, Charlestown, Mass

⁶ Home Base Program, a Red Sox Foundation and Massachusetts General Hospital Program, Charlestown, Mass

⁷ Crown Family School of Social Work, Policy, and Practice, University of Chicago, Chicago, Ill

⁸ University of Twente, RAM Group, EEMCS, Enschede, the Netherlands

Received December 4, 2023; revision requested December 26; final revision received February 10, 2025; accepted February 14.

Address correspondence to: A. Diociani (email: andrea.diociani@gmail.com).

Funding: A. Diociani was partially supported by #NEXTGENERATIONEU (NGEU) and funded by the Ministry of University and Research (MUR), National Recovery and Resilience Plan (NRRP), and project MNESYS (PE00000006)—A multiscale integrated approach to the study of the nervous system in health and disease (DN. 1553 11.10.2022).

Author contributions: Guarantors of integrity of entire study, **A. Diociani, M.A.I., A. Dua, R.G.**; study concepts/study design or data acquisition or data analysis/interpretation, all authors; manuscript drafting or manuscript revision for important intellectual content, all authors; approval of final version of submitted manuscript, all authors; agrees to ensure any questions related to the work are appropriately resolved, all authors; literature research, **A. Diociani, M.A.I., S.S., E.J.L., A. Dua, C.O.T.**; clinical studies, **M.A.I., E.J.L., C.W., R.G.**; experimental studies, **A. Diociani, C.O.T., R.G.**; statistical analysis, **A. Diociani, C.W., C.O.T.**; and manuscript editing, **A. Diociani, M.A.I., S.S., E.J.L., A. Dua, C.O.T., R.G.**

Disclosures of conflicts of interest: **A. Diociani** No relevant relationships. **M.A.I.** Serves as an unaffiliated neurotrauma consultant for the National Football League; receives travel support and honorariums for presentations at conferences and meetings. No relevant relationships. **S.S.** Internal research grant from Massachusetts General Hospital. **E.J.L.** No relevant relationships. **C.W.** No relevant relationships. **A. Dua** No relevant relationships. **C.O.T.** No relevant relationships. **R.G.** Scientific Advisory Board: Bayer HealthCare LLC, BrainTale, Agfa HealthCare; speaker honorarium: Siemens Medical Solutions, USA; research grant: Samsung Healthcare; consultant for Idorsia, Medtronic, and U.S. Attorney's Office, District of Colorado.

References

- Menon DK, Schwab K, Wright DW, Maas AI; Demographics and Clinical Assessment Working Group of the International and Interagency Initiative toward Common Data Elements for Research on Traumatic Brain Injury and Psychological Health. Position statement: definition of traumatic brain injury. *Arch Phys Med Rehabil* 2010;91(11):1637–1640.
- Michael AP, Stout J, Roskos PT, et al. Evaluation of Cortical Thickness after Traumatic Brain Injury in Military Veterans. *J Neurotrauma* 2015;32(22):1751–1758.
- Sharp DJ, Scott G, Leech R. Network dysfunction after traumatic brain injury. *Nat Rev Neurol* 2014;10(3):156–166.
- Elder GA, Gama Sosa MA, De Gasperi R, et al. Vascular and inflammatory factors in the pathophysiology of blast-induced brain injury. *Front Neurol* 2015;6:48.

5. Massaad E, Kiapour A. Long-Term Health Outcomes of Traumatic Brain Injury in Veterans. *JAMA Netw Open* 2024;7(2):e2354546.
6. Stone JR, Avants BB, Tustison NJ, et al. Functional and Structural Neuroimaging Correlates of Repetitive Low-Level Blast Exposure in Career Breachers. *J Neurotrauma* 2020;37(23):2468–2481.
7. Leiva-Salinas C, Singh A, Layfield E, Flors L, Patrie JT. Early Brain Amyloid Accumulation at PET in Military Instructors Exposed to Subconcussive Blast Injuries. *Radiology* 2023;307(5):e221608.
8. Tanaka SC, Yamashita A, Yahata N, et al. A multi-site, multi-disorder resting-state magnetic resonance image database. *Sci Data* 2021;8(1):227.
9. Blevins CA, Weathers FW, Davis MT, Witte TK, Domino JL. The Post-traumatic Stress Disorder Checklist for DSM-5 (PCL-5): Development and Initial Psychometric Evaluation. *J Trauma Stress* 2015;28(6):489–498.
10. Kroenke K, Strine TW, Spitzer RL, Williams JBW, Berry JT, Mokdad AH. The PHQ-8 as a measure of current depression in the general population. *J Affect Disord* 2009;114(1-3):163–173.
11. Cicerone KD, Kalmar K. Persistent postconcussion syndrome: The structure of subjective complaints after mild traumatic brain injury. *J Head Trauma Rehabil* 1995;10(3):1–17.
12. Modica LCM, Egnoto MJ, Statz JK, Carr W, Ahlers ST. Development of a Blast Exposure Estimator from a Department of Defense-Wide Survey Study on Military Service Members. *J Neurotrauma* 2021;38(12):1654–1661.
13. Whitfield-Gabrieli S, Nieto-Castanon A. Conn: a functional connectivity toolbox for correlated and anticorrelated brain networks. *Brain Connect* 2012;2(3):125–141.
14. Friston KJ, Ashburner JT, Kiebel SJ, Nichols TE, Penny WD, eds. *Statistical Parametric Mapping: The Analysis of Functional Brain Images*. Elsevier, 2007.
15. Nieto-Castanon A. *Handbook of functional connectivity Magnetic Resonance Imaging Methods in CONN*. Boston, Mass: Hilbert Press, 2020.
16. Edlow BL, Bodien YG, Baxter T, et al. Long-Term Effects of Repeated Blast Exposure in United States Special Operations Forces Personnel: A Pilot Study Protocol. *J Neurotrauma* 2022;39(19-20):1391–1407.
17. Nieto-Castanon A. Brain-wide connectome inferences using functional connectivity MultiVariate Pattern Analyses (fc-MVPA). *PLOS Comput Biol* 2022;18(11):e1010634.
18. Worsley KJ, Marrett S, Neelin P, Vandal AC, Friston KJ, Evans AC. A unified statistical approach for determining significant signals in images of cerebral activation. *Hum Brain Mapp* 1996;4(1):58–73.
19. Vedaie F, Mashhadi N, Alizadeh M, et al. Deep learning-based multimodality classification of chronic mild traumatic brain injury using resting-state functional MRI and PET imaging. *Front Neurosci* 2024;17:1333725.
20. Harnett NG, van Rooij SJH, Ely TD, et al. Prognostic neuroimaging biomarkers of trauma-related psychopathology: resting-state fMRI shortly after trauma predicts future PTSD and depression symptoms in the AURORA study. *Neuropsychopharmacology* 2021;46(7):1263–1271.
21. Zhang A, Wang X, Li J, et al. Resting-State fMRI in Predicting Response to Treatment With SSRIs in First-Episode, Drug-Naive Patients With Major Depressive Disorder. *Front Neurosci* 2022;16:831278.
22. Haran FJ, Zampieri C, Wassermann EM, et al. Chronic Effects of Breaching Blast Exposure on Sensory Organization and Postural Limits of Stability. *J Occup Environ Med* 2021;63(11):944–950.
23. Li MJ, Huang SH, Huang CX, Liu J. Morphometric changes in the cortex following acute mild traumatic brain injury. *Neural Regen Res* 2022;17(3):587–593.
24. Kou Z, Wu Z, Tong KA, et al. The role of advanced MR imaging findings as biomarkers of traumatic brain injury. *J Head Trauma Rehabil* 2010;25(4):267–282.
25. Shively SB, Horkayne-Szakaly I, Jones RV, Kelly JP, Armstrong RC, Perl DP. Characterisation of interface astroglial scarring in the human brain after blast exposure: a post-mortem case series. *Lancet Neurol* 2016;15(9):944–953.
26. Crombie KM, Ross MC, Letkiewicz AM, Sartin-Tarm A, Cisler JM. Differential relationships of PTSD symptom clusters with cortical thickness and grey matter volumes among women with PTSD. *Sci Rep* 2021;11(1):1825.
27. Gaggi NL, Ware JB, Dolui S, et al. Temporal dynamics of cerebral blood flow during the first year after moderate-severe traumatic brain injury: A longitudinal perfusion MRI study. *Neuroimage Clin* 2023;37:103344.
28. Bao W, Gao Y, Cao L, et al. Alterations in large-scale functional networks in adult posttraumatic stress disorder: A systematic review and meta-analysis of resting-state functional connectivity studies. *Neurosci Biobehav Rev* 2021;131:1027–1036.
29. Silva MA. Review of the Neurobehavioral Symptom Inventory. *Rehabil Psychol* 2021;66(2):170–182.
30. Belanger HG, Silva MA, Donnell AJ, McKenzie-Hartman T, Lamberty GJ, Vanderploeg RD. Utility of the Neurobehavioral Symptom Inventory As an Outcome Measure: A VA TBI Model Systems Study. *J Head Trauma Rehabil* 2017;32(1):46–54.
31. Koenigs M, Barbey AK, Postle BR, Grafman J. Superior parietal cortex is critical for the manipulation of information in working memory. *J Neurosci* 2009;29(47):14980–14986.
32. Kumral E, Çetin FE, Özdemir HN. Cognitive and Behavioral Disorders in Patients with Superior Parietal Lobule Infarcts. *Can J Neurol Sci* 2023;50(4):542–550.
33. Gilmore CS, Camchong J, Davenport ND, et al. Deficits in Visual System Functional Connectivity after Blast-Related Mild TBI are Associated with Injury Severity and Executive Dysfunction. *Brain Behav* 2016;6(5):e00454.
34. Cavanna AE, Trimble MR. The precuneus: a review of its functional anatomy and behavioural correlates. *Brain* 2006;129(Pt 3):564–583.
35. Lacey S, Lin JB, Sathian K. Object and spatial imagery dimensions in visuo-haptic representations. *Exp Brain Res* 2011;213(2-3):267–273.
36. Abdul Rahman MR, Abd Hamid AI, Noh NA, et al. Alteration in the Functional Organization of the Default Mode Network Following Closed Non-severe Traumatic Brain Injury. *Front Neurosci* 2022;16:833320.
37. Cattaneo Z, Lega C, Ferrari C, et al. The role of the lateral occipital cortex in aesthetic appreciation of representational and abstract paintings: a TMS study. *Brain Cogn* 2015;95:44–53.
38. Mayer AR, Mannell MV, Ling J, Gasparovic C, Yeo RA. Functional connectivity in mild traumatic brain injury. *Hum Brain Mapp* 2011;32(11):1825–1835.
39. Iraj A, Benson RR, Welch RD, et al. Resting State Functional Connectivity in Mild Traumatic Brain Injury at the Acute Stage: Independent Component and Seed-Based Analyses. *J Neurotrauma* 2015;32(14):1031–1045.